NANO LETTERS

LETTER

pubs.acs.org/NanoLett

Expanding the Optical Trapping Range of Lipid Vesicles to the Nanoscale

Poul M. Bendix and Lene B. Oddershede*

Niels Bohr Institute, The University of Copenhagen, Blegdamsvej 17, DK-2100 Copenhagen

Supporting Information

ABSTRACT: Small unilamellar lipid vesicles with diameters down to 50 nm enclosing high refractive index sucrose cores can be optically trapped individually in three dimensions using a focused laser beam. Combined optical trapping and confocal microscopy allows for simultaneous quantitative measurements of the forces exerted on individual vesicles and of their size and shape. The position of individual vesicles in three dimensions is measured with nanometer spatial and ~10 μs temporal resolution.

KEYWORDS: Optical trapping, lipid vesicles, liposomes, nanoparticles, force spectroscopy, position detection

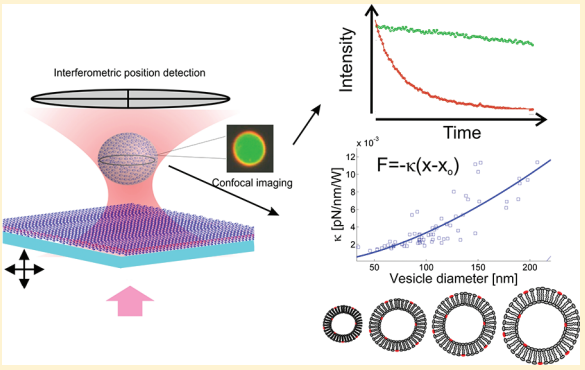

Naturally occurring lipid vesicles are the most commonly used carriers inside living organisms. Therefore, designed lipid containers and different types of liposomes hold great promise as nanocontainers for drug-delivery assays.[1−3] To understand vesicle transport and delivery, for example, in the synaptic region, and to develop efficient drug-delivery-containers, it is desirable to be able to optically control individual vesicles and to measure the distances they travel or the forces exerted on them by the cellular machinery. Also, for exploring molecular interactions involving membrane proteins both inside a living cell or in reconstituted assays, it is highly desirable to be able to optically manipulate individual liposomes and quantitatively measure interaction potentials, as commonly done using optical trapping of solid dielectric particles. Optical traps have been quite successful in unraveling the function of individual biomolecules.[4,5] This has most often been done *in vitro* using a micrometer-sized polystyrene bead as force transducer. However, *in vitro* measurements often face the criticism that experimental conditions are too far from the physiological. Therefore, the next natural step is to take the single molecule manipulation techniques inside the living cell and monitor the actions of cellular machines in their native environment. To this end, it will be advantageous to avoid having a hard micrometer-sized polystyrene sphere near the delicate biological molecules; it would be beneficial rather to use smaller force-transducers for precise force−distance measurements, transducers whose chemical and physical properties more resemble that of the cytoplasm. A lipid vesicle or a liposome is an obvious candidate as a force transducer in a biological nanoscopic assay. As proteins and molecules of interest can be readily reconstituted in the membrane, or encapsulated within the vesicle lumen, a vesicle-based force transducer will facilitate, for example, ultrasensitive and fast measurements of intermolecular interaction potentials.

Vesicles are soft shell-like structures made of lipid bilayers having index of refraction, $n_{lip} = 1.48$ (measured at $\lambda = 632$ nm),[6] which is significantly higher than the refractive index of water, $n_w = 1.33$, thus enabling optical trapping of lipid systems in three-dimension (3D) using a focused laser. Large vesicles with diameters 5−10 μm have been reported optically manipulated,[7] and somewhat smaller vesicles, down to 600 nm in diameter, have been investigated by optical trapping Raman microscopy.[8,9] Also single secretory vesicles with diameters of 1 μm have been investigated by combined optical trapping and electrophoresis separation.[10] A prerequisite for optical trapping is that a dipole moment can be induced in the trapped object. The larger the inducible dipole moment, the larger the gradient force responsible for optical confinement. Because the induced dipole moment scales with particle volume for small particles, optical trapping of nanoscopic objects poses a challenge. Polymeric nanoparticles[11] and in particular metallic nanoparticles have a relatively large inducible dipole moment, and optical trapping in 3D of metallic nanoparticles with sizes down to 10 nm has been reported.[12−15] To our knowledge, optical control and quantitative force measurements of small unilamellar vesicles (SUVs) has not been reported. This lack in literature probably originates from the fact that SUVs have a relatively small inducible dipole moment as they only consist of a thin membranous shell enclosing an aqueous volume, hence, they are difficult to trap. Moreover, lipid vesicle preparations are naturally polydisperse in

Received: September 14, 2011
Revised: November 2, 2011

dx.doi.org/10.1021/nl203200g | *Nano Lett.* XXXX, XXX, 000–000

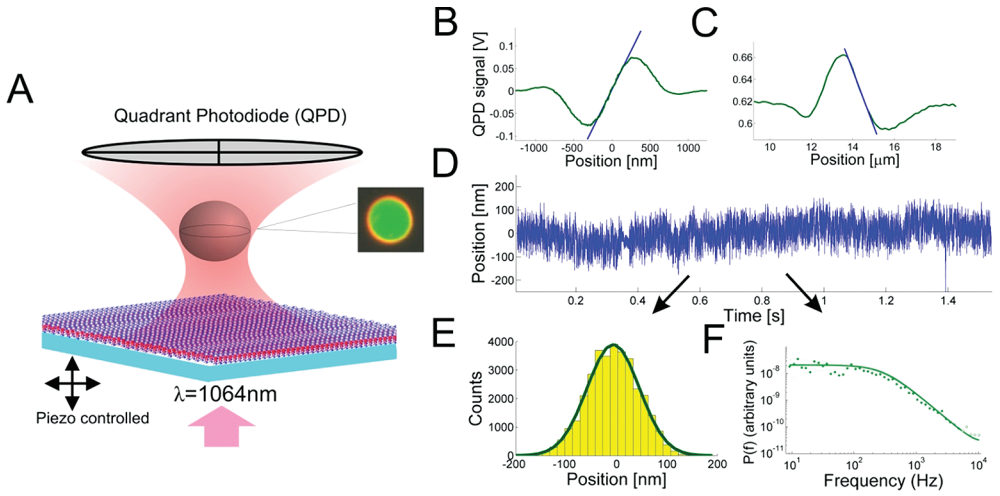

Figure 1. Illustration of the optical trapping configuration and the calibration procedure for a trapped vesicle. (A) A diffraction limited infrared laser spot confines a vesicle loaded with sucrose. The inset shows a confocal microscopy image of an optically trapped GUV whose membrane is labeled by TR-DHPE (red), its lumen is labeled by AH (green). (B) Plot of quadrant photodiode difference signal as a micrometer-sized vesicle immobilized on a supported lipid bilayer is moved in the lateral direction through the focus. (C) Plot of quadrant photodiode sum signal as a vesicle immobilized on a supported lipid bilayer is moved along the optical axis through the focus. (D) Positional time series of an optically trapped vesicle (d = 50 nm, P = 850 mW) containing 1 M sucrose. (E) Histogram of positions visited by the d = 50 nm trapped vesicle, full line shows a Gaussian fit to the data. (F) Power spectrum of the time series shown in D (f_c = 299 Hz ± 8 Hz), full line shows a Lorentzian fit (done by Matlab procedures of ref 24).

size, hence, for vesicles below the diffraction limit it is not trivial to quantify the size of each trapped vesicle. This quantification is needed for the most commonly used force calibration procedures.

By using an optimized optical trapping assay in combination with simultaneous confocal microscopy, we optically trapped individual nanoscale SUVs, loaded with a highly concentrated sucrose solution, in 3D using a focused laser beam. The size of vesicles smaller than the diffraction limit was obtained by quantitative confocal fluorescence imaging. Vesicles with sizes comparable to the laser focus were used to assess the effect of the trapping laser on the mechanical stability of the bilayer and on the labeling fluorophores. There was no significant deformation of optically trapped vesicles containing sucrose cores, even at high laser powers. The high index sucrose core caused efficient scattering and refraction of laser light that allowed for back focal plane detection of the vesicle position in 3D by using a quadrant photodiode providing a very high temporal and spatial resolution. We also performed the force calibration using an image-based method. Finally, as a proof of principle, we demonstrated how to use an optically trapped vesicle to probe the interaction between a ligand and its substrate.

The experimental setup allowing simultaneous optical trapping and fluorescent confocal detection is achieved by coupling a Nd:YVO_4 (5 W Spectra Physics BL106C, λ = 1064 nm, TEM_{oo}) laser into the Hg lamp entrance of a Leica SP5/TCS confocal laser scanning microscope. Details of the setup is described in ref 16. The laser was focused through a high numerical aperture oil immersion objective (Leica HCX, PL APO, 100×, NA = 1.4, oil). To minimize spherical aberration and improve optical trapping, we used an immersion oil with refractive index n = 1.55, which provides an optimal focus 5−10 μm from the glass coverslip surface.[17] All laser powers noted are measured at the sample using the dual objective method.[18] The position of the focus relative to the sample was accurately controlled using a three-dimensional piezoelectric stage (PI 731.20, Physik Instrumente, Germany). Stokes drag experiments were performed by oscillating the stage with a triangular wave while keeping the laser focus at a fixed position.

Fast position detection was performed using a quadrant photodiode (S5981, Hamamatsu) collecting the forward scattered light from the vesicle. Axial position detection was significantly improved by reducing the numerical aperture of the condenser to approximately 30%.[19] Optically trapped lipid vesicles were imaged using a confocal laser scanning with λ = 488 nm for exiting Alexa Hydrazide 488 (AH) and dilinoleyloxacarbocyanine perchlorate (DiO), (Molecular Probes, Eugene, OR) or scanning with λ = 594 nm for exciting 1,2-dipalmitoyl-sn-glycero-3-phosphoethanolamine-N-1-Texas Red hexanoyl (TR-DHPE) (Molecular Probes, Eugene, OR). The emitted light from the fluorophores was collected using photomultiplier tubes. A pinhole of 1 airy was used to reject light out of focus. The glass substrate was passivated by standard protocols as detailed in Supporting Information.

The vesicles were composed of 80% dioleoylphosphatidylcholine (DOPC), 18% dioleoylphosphatidylglycerol (DOPG) purchased from Avanti Polar Lipids, Inc. (Alabaster, AL) and 2% lipophilic dyes, either TR-DHPE or DIO. Encapsulation was achieved by hydration of the lipid film with aqueous sucrose solution with or without AH for labeling the interior solution. This hydration step results in giant unilamellar vesicles (GUVs) that were subsequently extruded using polycarbonate filters with pore sizes of 50 nm, 100 nm, or 1 μm (Avanti Polar Lipids, Inc. Alabaster, AL). The lipid concentration in the vesicle preparation was 1 mg/mL. Depending on the extrusion pore size we subsequently diluted the vesicle stock between 1000× and 10 000× before the experiments with PBS buffer containing NaCl at a concentration iso-osmolar with the sucrose solution. The volume of the vesicle is preserved due to very low membrane permeability of sucrose across the bilayer membrane. Deformation of the vesicle (and hence a volume change) would cause an osmotic imbalance and result in stretching of the bilayer that

dx.doi.org/10.1021/nl203200g |*Nano Lett.* XXXX, XXX, 000–000

is approximately 4 orders of magnitude more energy costly than bending a lipid bilayer (bending modulus of a membrane $\sim 20 k_B T$).

In any translational direction an optical trap exerts a harmonic force, $F = -\kappa \Delta x$, where Δx is the deviation from the equilibrium position and κ is the spring constant characterizing the optical trap. Figure 1a shows a sketch of a vesicle in an optical trap, the inset shows a confocal picture of a trapped vesicle, the membrane is labeled by TR-DHPE (red) and the lumen by AH (green). The forward scattered trapping laser light is collected by a quadrant photodiode (QPD). A prerequisite of standard optical trapping calibration protocols is that the voltage signal from the photodetection system is linearly proportional to the displacement of the object in the trap. For instance, the lateral coordinate x is found by $x \propto (A + B) - (C + D)$, where A, B, C, and D denote the voltages detected in each of the four quadrants,[20,21] and the position along the axial direction, z, is found by $z \propto A + B + C + D$.[22] These relations should apply to any spherical dielectric scatterer. In order to test whether these relations also hold true for a trapped vesicle, we translated a vesicle immobilized on a supported lipid bilayer through the laser focus at constant velocity while measuring the output from the photodiode. The resulting difference signal, corresponding to the x direction, is shown in Figure 1b, the sum signal (z direction) is shown in Figure 1c. There is clearly a linear region (~ 1 μm in the axial direction, ~ 500 nm in the lateral direction) confirming a one-to-one correspondence between voltage output and vesicle position; thus, the standard optical trapping detection protocols also apply to systems where a lipid vesicle is used as the force-transducing handle.

Time series of the positions visited by an optically trapped vesicle were recorded over 3 s with a sampling frequency of $f_{sample} = 22$ kHz, a time series of the positions visited by a trapped $d = 50$ nm vesicle is shown in Figure 1d, the corresponding Gaussian position histogram is shown in Figure 1e. The dynamics in one dimension of an optically trapped object is well described by the Langevin equation, $F(T,t) = \kappa x + \gamma v$, where γ is the Stokes drag coefficient, $\gamma = 6\pi\eta R$ (η being the viscosity of water and R vesicle radius) if far from any surfaces, $F(T,t)$ is a stochastic force, typically modeled as white noise, which is dependent on temperature, T, and time, t.[20,23] The positional power spectrum is well fitted by a Lorentzian function, $S_x = k_B T/(\gamma \pi^2 (f_c^2 + f^2))$, where $f_c = \kappa/2\pi\gamma$ is denoted the corner frequency. This formalism was incorporated in a Matlab program[24] that also took into account the filtering effect of the photodiode[25] and returned the spring constant of the optical trap, κ. Figure 1f shows the power spectrum of the lateral time series shown in Figure 1d for a $d = 50$ nm vesicle, the Lorentzian fit is shown as a full line. Two examples of power spectra for axial time series taken with different laser powers are shown in Supporting Information Figure S1, which also verifies the expected proportionality between the axial κ and laser power.

The size of an optically trapped vesicle smaller than or similar to the diffraction limit was quantified from the emission of the membrane incorporated fluorophore. The emitted intensity, I, and vesicle radius, R, are related as $I = kR^2$, where k is a constant. k is found from the relation $k = \langle I \rangle / \langle R \rangle^2$, where $\langle R \rangle$ is the average vesicle diameter found by dynamic light scattering (DLS), see Supporting Information Figure S2, and $\langle I \rangle$ is the corresponding average intensity measured on a large number of trapped vesicles from the ensemble used for DLS.[26] The inset of Supporting InformationFigure S2 shows a control where the fluorescence of surface attached vesicles was quantified, the resulting curve resembled the DLS curve with a single maximum and a similar shape.

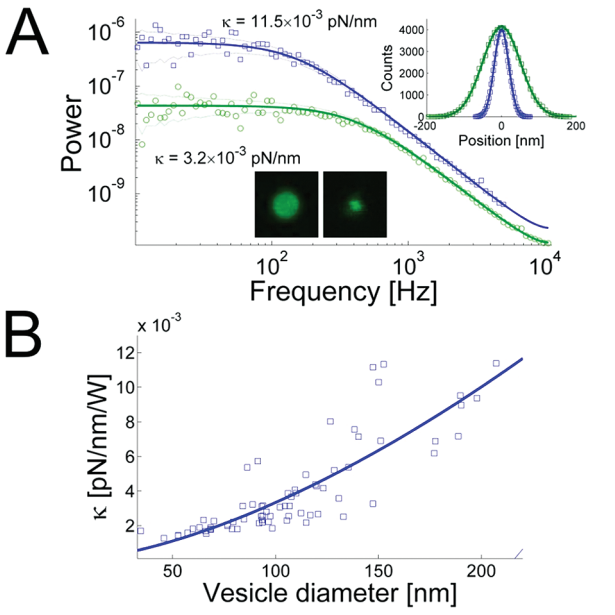

Figure 2. Optical trapping strength correlates with vesicle size. (A) Power spectra from two optically trapped lipid vesicles of different sizes (blue squares, $d = 1.2$ μm, $P = 170$ mW, $\kappa = 11.5 \times 10^{-3}$ pN/nm; green circles, $d = 130$ nm, $P = 850$ mW, $\kappa = 3.2 \times 10^{-3}$ pN/nm). Inset shows confocal images of the two vesicles (membrane labeled with DiO). (B) κ (normalized by laser power) as a function of vesicle diameter for $n = 71$ vesicles. Full line shows a fit of $\kappa \propto R^{1.6}$ to data.

Small vesicles extruded at 50 or 100 nm and containing sucrose were individually trapped by random diffusion into the trap. The vesicle concentration was adjusted such that the typical waiting time for a vesicle to enter the trap (typically several minutes) was significantly longer than the data acquisition time (3 s). Both water-containing vesicles and vesicles filled by sucrose could be optically trapped. However, in accordance with observations from trapping of larger vesicles,[7] vesicles without sucrose proved significantly more difficult to trap than vesicles with sucrose (see Supporting Information Videos 1 and 2). This is because the refractive index of 1 M sucrose (as predominantly used in the present work) is $n = 1.38$, which is significantly higher than that of water ($n = 1.33$). Micron-sized vesicles loaded with sucrose could be efficiently trapped at low laser powers ~ 10 mW whereas smaller sucrose loaded vesicles having diameters between 50−200 nm required laser powers of hundreds of milliwatts for optical trapping. Also, the sucrose-filled vesicles gave a significantly stronger signal on the photodiode. Therefore, and because several biologically relevant vesicles, for instance the large dense-core vesicles (LDCV) responsible for hormone secretion with a condensated protein core containing up to 500−1000 mM adrenalin, have a high osmolarity and an index of refraction comparable to that of sucrose, in the following we focus on optical trapping of vesicles containing 1 M sucrose.

The effect of particle size on trapping efficiency is clearly demonstrated in Figure 2a for a $d = 130$ nm vesicle (green data) and a $d = 1.2$ μm vesicle (blue data). From the power spectra shown in Figure 2a, κ for the larger vesicle was found to be roughly four times larger than κ for the smaller vesicle, despite

dx.doi.org/10.1021/nl203200g |Nano Lett. XXXX, XXX, 000–000

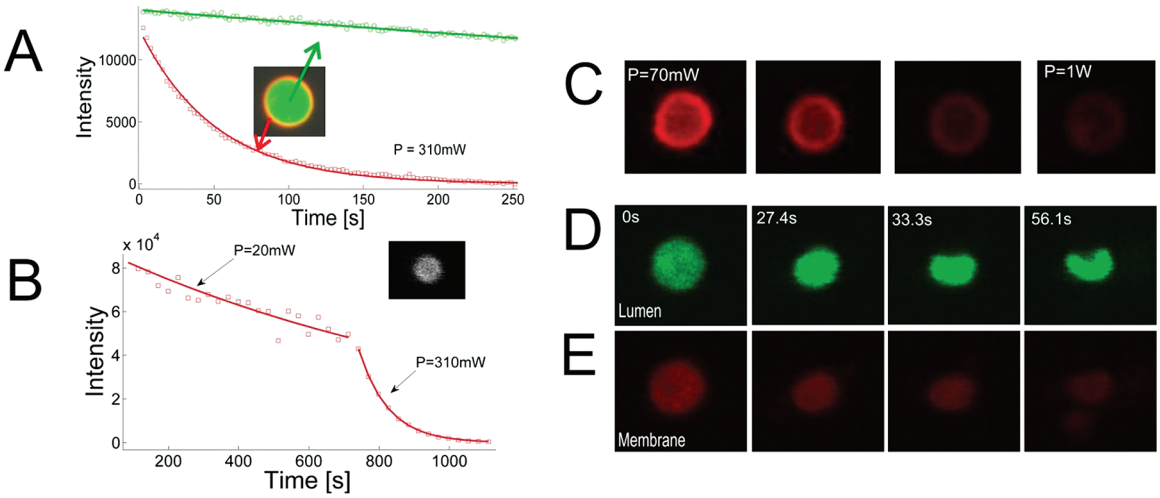

Figure 3. Effect of trapping laser on bleaching rates and vesicle shape. (A) Intensity of membrane incorporated TR-DHPE and AH in the vesicle lumen as a function of time during optical trapping. The two fluorophores have distinct bleaching rates ($\tau^{-1} = 7.0 \times 10^{-4} \pm 3.1 \times 10^{-5} s^{-1}$ for AH and $\tau^{-1} = 0.01 \pm 4.1 \times 10^{-4} s^{-1}$ for TR-DHPE). (B) Intensity of membrane incorporated TR-DHPE as a function of time for an optically trapped vesicle while increasing power from $P = 20$ mW to $P = 310$ mW. The bleaching rates of at the two different laser powers are $\tau_1^{-1} = 8.6 \times 10^{-4} \pm 1.7 \times 10^{-4}\ s^{-1}$ and $\tau_2^{-1} = 0.01 \pm 2.4 \times 10^{-4}\ s^{-1}$, respectively. (C) Effect of increasing laser power on the shape of a $d \sim 1\ \mu$m vesicle loaded with 1 M sucrose. Laser power is increased from 70 mW to 1 W. Significant bleaching is observed for the TR-DHPE fluorophore but no measurable deformation. (D + E) A $d \sim 1\ \mu$m vesicle with an aqueous (no sucrose) core initially trapped at $P = 170$ mW (left images). At $t = 27.5$ s, the laser power is increased to 850 mW and significant deformation of the vesicle is observed at subsequent times; the AH labeled lumen is shown in (D) and the TR-DHPE labeled membrane is shown in (E).

the fact that a laser power of $P = 170$ mW was used to trap the larger vesicle and a laser power of $P = 850$ mW was used to trap the smaller vesicle. The resulting position distribution is consequently narrower for the larger vesicle as seen in the inset to Figure 2a. The trapping constant κ was quantified for each vesicle (as described above) and an image was acquired to determine its size.

We found corresponding values of κ and size for a number of SUVs; the results are shown in Figure 2b. κ scales with laser power, hence, in order to compare κ obtained at different laser powers, the value of κ plotted in Figure 2b is normalized by laser power. Vesicles ranging in size from approximately 40 to 200 nm show an increase of κ with size. The measured scaling relation, $\kappa \sim R^{1.6}$, differs from a scaling with particle volume, $\kappa \sim R^3$, as observed for solid Rayleigh particles.[11,13,14] It is well-known that sucrose encapsulation efficiency decreases with vesicle size,[27] therefore, a scaling exponent lower than 3 is expected for optical trapping of sucrose loaded vesicles. For the larger vesicles the data do appear relatively spread. This could be due to imprecision in size determination caused by an inhomogeneous distribution of fluorophores among the vesicles, or because some of the vesicles are oligolamellar (contain one or several internal vesicles) that would influence trapping strength and lead to an overestimation of vesicle size.

As the vesicles were trapped using relatively high laser powers, a potential degradation of the fluorescent markers could occur even though the wavelength of the trapping laser was far from the peak absorption of the fluorescent molecule.[28] A pronounced bleaching during the experiment could lead to an underestimate of vesicle size. We quantified the bleaching rate of the fluorophores used to label the vesicles, TR-DHPE, DiO, and AH. Figure 3a (red curve) shows the bleaching rate of TR-DHPE at relatively high laser powers, $P = 310$ mW. Bleaching rates for DiO were similar to those of TR-DHPE. AH inside a vesicle trapped with $P = 310$ mW (green curve in Figure 3a) bleaches more slowly than the membrane markers (TR-DHPE and DiO), after several minutes still ~90% of the maximum AH signal prevails.

The bleaching rate is strongly dependent on trapping laser power. This is shown in Figure 3b where the intensity of membrane bound TR-DHPE is plotted as a function of time. The vesicle was initially is trapped at $P = 20$ mW and after ~10 min laser power was increased to 310 mW. Clearly, the TR-DHPE signal decreases more rapidly at high laser powers. This experiment demonstrates that the trapping laser and not the imaging laser is predominantly responsible for fluorophore bleaching. Bleaching of the membrane markers leads to an under estimation of the vesicle size. This error was minimized by acquiring the confocal image for size determination within the first 3 s of vesicle trapping. From the measured decay constant, we estimated the corresponding error in vesicle size determination to be up to 3% (using a relatively high 310 mW laser power).

The power level used to trap the smallest vesicles in Figure 2b has previously been shown to be sufficient to bend bilayers or deform vesicles, albeit, at shorter a wavelength.[29] We did not observe any laser induced deformation of vesicles containing 1 M sucrose, a series of confocal images of a TR-DHPE labeled sucrose loaded vesicle trapped while increasing the laser power up to $P = 1$ W is shown in Figure 3c (and in Supporting Information Video 3). Vesicles that self-assembled in pure water and therefore contained only pure water deformed more easily. Left images in Figures 3d and 3e show a vesicle with an aqueous core trapped at $P = 170$ mW, subsequent pictures show significant deformation after the laser power at $t = 27.4$ s is raised to $P = 850$ mW (Figure 3d shows AH labeled lumen, Figure 3e shows TR-DHPE labeled membrane). Furthermore, optical trapping of a vesicle having the same index of refraction inside as outside results in trapping of the lipid bilayer (see Supporting Information Video 4).

dx.doi.org/10.1021/nl203200g |*Nano Lett.* XXXX, XXX, 000–000

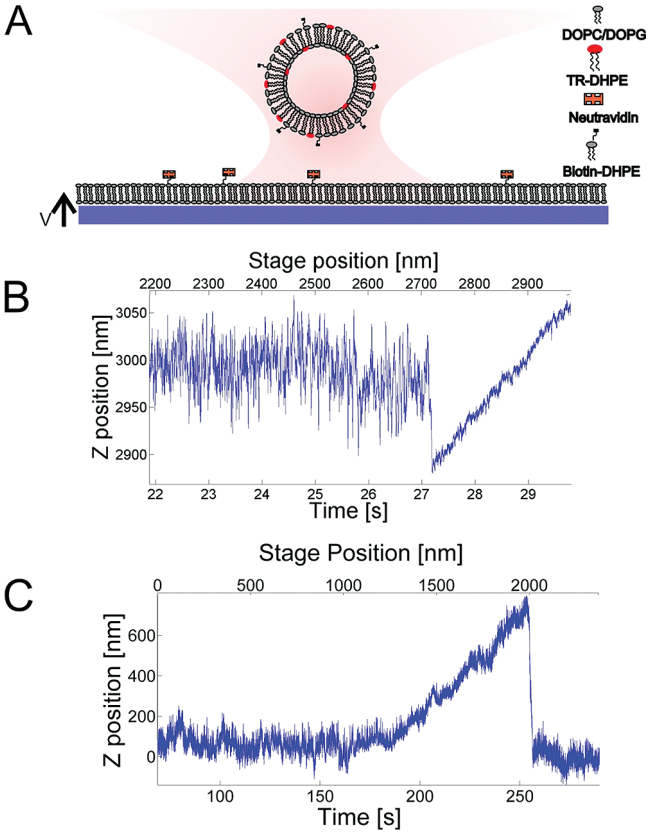

Figure 4. Probing of specific and unspecific intermembrane interactions using an optically trapped vesicle. (A) An optically trapped vesicle containing lipid-anchored biotin molecules approaches a supported lipid bilayer containing neutravidin molecules. (B) The axial positions visited by an optically trapped ∼1 μm biotinylated vesicle approaching a neutravidin-coated supported lipid bilayer at constant speed (100 nm/s). At 27 s, the biotinylated bead jumps and irreversibly binds to the neutravidin. (C) Control experiment showing axial positions visited by an optically trapped ∼2 μm biotinylated vesicle approaching a supported lipid bilayer (without neutravidin) at constant speed. At ∼180 s, the surface encounters the particle; at ∼250 s, the surface is lowered with respect to the optical trap and the particle resumes Brownian motion. The vesicle does not jump and does not stick irreversibly to the surface; only steric repulsion was present between the two bilayers. Axes in (B) and (C) are relative, not absolute.

The deformation, Δb, of an optically trapped lipid vesicle of conserved volume containing a sucrose core is derived in ref 30 (and detailed in Supporting Information)

$$\Delta b = \frac{n_w P Q}{\pi c Y T}$$

where $Q = Q_{back} + Q_{front}$ with Q_{back} and Q_{front} being the fractions of momentum transferred at the back and front side of the vesicle, respectively. n_w is the refractive index of water, c is the speed of light, Y is Young's modulus (=10^7 N/m for bilayers[31]), and T is the membrane thickness (T = 5 nm). Hence, the deformation is linearly proportional to the total power incident on the vesicle. Typical high powers for trapping the larger vesicles used in this work were P = 50−100 mW, which should lead to deformations on the order of 1 nm for vesicles filled with 1 M of sucrose, a nonobservable deformation. The smaller vesicles have optical cross sections significantly smaller than the laser focus so the effective power becomes much lower than the total power passing through the focus, thus resulting in a nonobservable deformation.

The strength of an optical trap can alternatively be calibrated through image analysis using the "Stokes-drag" calibration method (detailed in Supporting Information). Using low-trapping laser powers SUVs can be imaged for extended periods of time, especially if imaged by AH emission. In the Stokes-drag method, the bead is exposed to a constant drag and its displacement from the equilibrium position is measured by image analysis. Supporting Information Figure S3 shows the positions visited by an optically trapped bead while moving the piezo-stage at constant speed by a triangular wave. By measuring the amplitude of the bead's motion, κ can be extracted (as detailed in Supporting Information). For the same vesicle, we used both the photodiode and image-based analyses to determine the positions visited at three different trapping laser powers (data shown in Supporting Information Figure S4). Both methods yield the same amplitudes, within the uncertainties, and the same κ too, though a higher precision was reached by the photodiode based method than by the image-based method.

Optical trapping of vesicles will prove useful for probing membrane associated proteins during intermembrane interactions, as for instance mediated by the SNARE complex.[32,35] As a proof of principle, we here show that an optically trapped vesicle with membrane incorporated biotin molecules approaching a supported lipid bilayer with neutravidin molecules can be used to probe the biotin−neutravidin interaction. A sketch of the experiment is shown in Figure 4a. For this experiment, a geometry was chosen where the interaction potential was probed in a direction along the propagating laser beam, the axial direction, hence, the trap needed calibration in the axial direction (as shown in Supporting Information Figure S1). The axial positions visited by the vesicle with respect to the focus of the optical trap is shown in Figure 4b. First, the bead performs normal Brownian motion in the trap while approaching the surface at a constant speed. Suddenly, around 27 s, the biotinylated particle jumps to the neutravidin surface. After this jump, the particle irreversibly sticks to the surface, its Brownian motion ceases, and it follows with the surface as it is moved at constant speed toward and through the trap focus. Figure 4c illustrates a control experiment where a biotinylated vesicle approaches a lipid bilayer (without neutravidin). This particle performs normal Brownian fluctuations in the trap too. At ∼180 s the surface, which is moved at constant speed toward the particle, collides with the particle and pushes the particle upward in the trap. At around 250 s, the surface is lowered with respect to the trap and the particle resumes it previous Brownian fluctuations in the trap; hence, it did not attach to the surface. Other differences between the specific interaction shown in Figure 4b and the control in Figure 4c are, for instance, that in the control there is no distinct jump to the surface and the particle exhibits thermal fluctuations even while being pushed upward through the focus by the approaching surface. In principle, the underlying nanoscale interactions can be found by measuring the distribution of vesicle jumps to the surface[33] or by measuring the shift of the positions visited within the optical trap.[34]

An optical trap is weakest in the axial direction, hence, this is well suited for probing of soft long-range interaction potentials. The lateral potential is typically twice as strong as the axial potential. Hence, larger forces can be exerted and measured in the lateral directions. We explored the maximum lateral strength of liposome trapping by measuring the force at which a 2.2 μm

dx.doi.org/10.1021/nl203200g |Nano Lett. XXXX, XXX, 000–000

liposome escaped the trap using an assay where the stage was oscillated in a controlled fashion while the laser power was gradually decreased. At 90 mW, the vesicle occasionally escaped the trap (as shown in Supporting Information Figure S5), this corresponding to a force of 4.1 pN. As the force is linearly proportional to laser power and we can ramp the power up to 900 mW or more, optical forces of 40 pN can easily be applied to a micrometer-sized vesicle.

We have shown that individual vesicles with diameters down to 50 nm can be optically trapped using an infrared CW laser and used as force-transducers for precise force and distance measurements. Forces of tens of picoNewtons can easily be applied on micrometer-sized vesicles containing sucrose. By combined optical trapping and confocal microscopy the trapping strength as well as the sizes of the individual vesicles were measured. The spring constant characterizing the optical trapping potential increased with vesicle size but scaled slower with size than solid Rayleigh particles do. Vesicles with a high refractive index sucrose core were significantly easier to trap than vesicles containing pure water. Also, the high viscosity sucrose core osmotically stabilized the shape of the vesicle and protected the vesicle against mechanical deformation due to optically induced stresses. Optical trapping with fast and precise position detection combined with confocal fluorescence imaging of vesicles could be useful for probing fast kinetics as well as interaction potentials of membrane bound proteins as for instance SNARE complexes.[32,35]

■ ASSOCIATED CONTENT

Supporting Information. Calculation of vesicle deformation, Stokes-drag calibration, Protocol for passivation of glass substrates. Figure S1: Power spectra and force calibration in the axial direction. Figure S2: Size distribution of extruded vesicles measured by dynamic light scattering measurement and by surface distribution. Figure S3: Image-based Stokes-drag calibration of an optically trapped vesicle. Figure S4: Comparison of photodiode detection and image-based detection of an optically trapped vesicle. Figure S5: Measurements of the maximum force exerted on a trapped liposome. Video 1: Vesicles with an aqueous core trapped by P = 170 mW, stage is oscillated at 0.5 Hz with an amplitude of 8 μm. κ = 0.0037 pN/nm/W. Video 2: Vesicles with a 1 M sucrose core trapped by P = 70 mW, stage is oscillated at 10 Hz with an amplitude of 8 μm. κ = 0.05 pN/nm/W. Video 3: A vesicle (diameter $\sim$ 1 μm) with a sucrose core is initially trapped at P = 70 mW. Laser power is subsequently increased to 1 W while the vesicle still shows no sign of deformation (same data is depicted in Figure 3c). Video 4: Optical trapping of a large vesicle (diameter $\sim$ 5 μm) with an aqueous core. The laser focus is marked by a red circle; it is clearly (only) the bilayer material which is trapped. This material is available free of charge via the Internet at http://pubs.acs.org.

■ AUTHOR INFORMATION

Corresponding Author

*E-mail: oddershede@nbi.dk.

■ ACKNOWLEDGMENT

We acknowledge fruitful discussions with Jakob B. Sørensen. This work was supported by the Carlsberg foundation and by MolPhysX University of Copenhagen Center of Excellence.

■ REFERENCES

(1) Volodkin, D. V.; Skirtach, A. G.; Mohwald, H. Near-IR Remote Release from Assemblies of Liposomes and Nanoparticles. *Angew. Chem.* **2009**, *48*, 1809.

(2) Cauda, V.; Engelke, H.; Sauer, A.; Arcizet, D.; Bräuchle, C.; Rädler, J.; Bein, T. Colchicine-Loaded Lipid Bilayer-Coated 50nm Mesoporous Nanoparticles Efficiently Induce Microtubule Depolymerization upon Cell Uptake. *Nano Lett.* **2010**, *10* (7), 2484–2492.

(3) Kluza, E.; Schaft, D. W. J.; Hautvast, P. A. I.; Mulder, W. J. M.; Mayo, K. J.; Griffioen, A. W.; Strijkers, G. J.; Nicolay, K. Synergistic Targeting of $\alpha_v\beta_3$ Integrin and Galectin-1 with Heteromultivalent Paramagnetic Liposomes for Combined MR Imaging and Treatment of Angiogenesis. *Nano Lett.* **2010**, *10* (1), 52–58.

(4) Guydosh, N. R.; Block, S. M. Direct observation of the binding state of the kinesin head to the microtubule. Guydosh and Block. *Nature* **2009**, *461*, 125–128.

(5) Veigel, C.; Schmidt, C. F. Moving into the cell: single-molecule studies of molecular motors in complex environment. *Nat. Rev. Mol. Cell Biol.* **2011**, *12*, 163–176.

(6) Jin, Y. L.; Chen, J. Y.; Xu, L.; Wang, P. N. Refractive index measurement for biomaterial samples by total internal reflection. *Phys. Med. Biol.* **2006**, *51*, N371–N379.

(7) Ichikawa, M.; Kenichi, Y. Optical transport of a single cell-sized vesicle. *Appl. Phys. Lett.* **2001**, *79* (27), 4598–4600.

(8) Cherney, D. P.; Conboy, J. C.; Harris, J. M. Optical-Trapping Raman Microscopy Detection of Single Unilamellar Lipid Vesicles. *Anal. Chem.* **2003**, *75* (23), 6621–6628.

(9) Cherney, D. P.; Bridges, T. E.; Harris, J. M. Optical Trapping of Unilamellar Phospholipid Vesicles: Investigation of the Effect of Optical Forces on the Lipid Membrane Shape by Confocal-Raman Microscopy. *Anal. Chem.* **2004**, *76* (17), 4920–4928.

(10) Chiu, D. T.; Lillard, S. J.; Scheller, R. H.; Zare, R. N.; Rodriguez-Cruz, S. E.; Williams, E. R.; Orwar, O.; Sandberg, M.; Lundqvist, J. A. Probing Single Secretory Vesicles with Capillary Electrophoresis. *Science* **1998**, *279* (5354), 1190–1193.

(11) Rohrbach, A. Stiffness of Optical Traps: Quantitative Agreement between Experiment and Electromagnetic Theory. *Phys. Rev. Lett.* **2005**, *95*, 168102.

(12) Svoboda, K.; Block, S. M. Optical trapping of metallic Rayleigh particles. *Opt. Lett.* **1994**, *19* (13), 930–932.

(13) Hansen, P. M.; Bhatia, V. K.; Harrit, N.; Oddershede, L. Expanding the Optical Trapping Range of Gold Nanoparticles. *Nano Lett.* **2005**, *5* (10), 1937–1942.

(14) Hajizadeh, F.; Reihani, S. N S. Optimized optical trapping of gold nanoparticles. *Opt. Expr.* **2010**, *18* (2), 551–559.

(15) Selhuber-Unkel, C.; Zins, I.; Schubert, O.; Soennichsen, C.; Oddershede, L. B. Quantitative optical trapping of single gold nanorods. *Nano Lett.* **2008**, *8* (9), 2998–3003.

(16) Richardson, A. C.; Reihani, N.; Oddershede, L. B. Combining confocal microscopy with precise force-scope optical tweezers. *Proc. of SPIE* **2006**, *6326*, 632628.

(17) Reihani, S. N. S.; Oddershede, L. Optimizing immersion media refractive index improves optical trapping by compensating spherical aberrations. *Opt. Lett.* **2007**, *32* (14), 1998–2000.

(18) Misawa, H.; Koshioka, M.; Sasaki, K.; Kitamura, N.; Masuhara, H. Three-Dimensional Optical Trapping and Laser Ablation of a Single Polymer Latex Particle in Water. *J. Appl. Phys.* **1991**, *70* (7), 3829–3836.

(19) Dreyer, J. K.; Berg-Sørensen, K.; Oddershede, L. Improved Axial Position Detection in Optical Tweezers Measurements. *Appl. Opt.* **2004**, *43* (10), 1991–1996.

(20) Gittes, F.; Schmidt, C. F. Interference model for back-focal-plane displacement detection in optical tweezers. *Opt. Lett.* **1998**, *23* (1), 7–9.

(21) Rohrbach, A. Three-dimensional position detection of optically trapped dielectric particles. *J. Appl. Phys.* **2002**, *91* (8), 5474–5488.

(22) Pralle, A.; Prummer, M.; Florin, E.-L.; Stelzer, E. H. K.; Hörber, J. K. H. Three-Dimensional High-Resolution Particle Tracking for Optical Tweezers by Forward Scattered Light. *Microsc. Res. Tech.* **1999**, *44*, 378–386.

(23) Berg-Sørensen, K.; Flyvbjerg, H. Power spectrum analysis for optical tweezers. *Rev. Sci. Instrum.* **2004**, *75* (3), 594–612.
(24) Hansen, P. M.; Tolic-Nørrelykke, I. M.; Flyvbjerg, H.; Berg-Sørensen, K. Tweezercalib 2.1: Faster version of a MatLab package for precision calibration of optical tweezers. *Comput. Phys. Commun.* **2006**, *175* (8), 572–573.
(25) Berg-Sørensen, K.; Oddershede, L.; Florin, E.-L.; Flyvbjerg, H. Unintended filtering in typical photo-diode detection system for optical tweezers. *J. Appl. Phys.* **2003**, *93* (6), 3167–3176.
(26) Kunding, A. H.; Mortensen, M. W.; Christensen, S. M.; Stamou, D. A fluorescence-based technique to construct size distributions from single object measurements, application to the extrusion of lipid vesicles. *Biophys. J.* **2008**, *95* (3), 1176–1188.
(27) Lohse, B.; Bolinger, P.-Y.; Stamou, D. Encapsulation efficiency measured on single small unilamellar vesicles. *J. Am. Chem. Soc.* **2008**, *130* (44), 14372.
(28) Dijk, M. A.; Kapitein, L. C.; Mameren, J.; Schmidt, C. F.; Peterman, E. J. G. Combining optical trapping and single-molecule fluorescence spectroscopy: enhanced photobleaching of fluorophores. *J. Phys. Chem. B* **2004**, *108* (20), 6479–6484.
(29) Bar-Ziv, R.; Moses, E.; Nelson, P. Dynamic Excitations in Membranes Induced by Optical Tweezers. *Biophys. J.* **1998**, *75* (1), 294–320.
(30) Møller, P. C. F.; Oddershede, L. B. Quantification of droplet deformation by electromagnetic trapping. *Eur. Phys. Lett.* **2009**, *88*, 48005.
(31) Evans, E.; Needham, D. Physical Properties of Surfactant Bilayer Membranes: Thermal Transitions, Elasticity, Rigidity, Cohesion, and Colloidal Interactions. *J. Phys. Chem.* **1987**, *91* (16), 4219–4228.
(32) Bogaart, G.; Holt, M. G.; Bunt, G.; Riedel, D.; Wouters, F. S.; Jahn, R. One SNARE complex is sufficient for membrane fusion. *Nat. Struct. Mol. Biol.* **2010**, *17* (3), 358–364.
(33) Dreyer, J. K.; Berg-Sørensen, K.; Oddershede, L. Quantitative approach to small-scale nonequilibrium systems. *Phys. Rev. E.* **2006**, *73*, 051110.
(34) Hansen, P. M.; Dreyer, J. K.; Ferkinghoff-Borg, J.; Oddershede, L. Novel optical and statistical methods reveal colloid-wall interactions inconsistent with DLVO and Lifshitz theories. *J. Colloid Interface Sci.* **2005**, *287*, 561–571.
(35) Brunger, A. T.; Weninger, K.; Bowen, M.; Chu, S. Single-Molecule Studies of the Neuronal SNARE Fusion Machinery. *Annu. Rev. Biochem.* **2009**, *78*, 903–928.